Desalination and Water Treatment
www.deswater.com

doi: 10.1080/19443994.2015.1035494

57 (2016) 9569–9584
May

Taylor & Francis
Taylor & Francis Group

CCD series no-16: opened vs. closed circuit SWRO batch desalination for volume reduction of Silica containing effluents under super-saturation conditions

Avi Efraty

Desalitech Ltd, P.O. Box 132, Har Adar 90836, Israel, email: avi@desalitech.com

Received 12 February 2014; Accepted 15 March 2015

ABSTRACT

Opened-circuit desalination (OCD) of a high salinity source (>10,000 ppm) also containing large amounts of Silica (>124 ppm) by the application of a single-element module batch apparatus under the conditions of fixed applied pressure of declined flux at low pH was reported to proceed with 80–85% recovery by a high-energy process of low permeate productivity through high super-saturation conditions of silica. The present study describes theoretical model simulations of OCD and closed-circuit desalination (CCD) processes of same feed source (10,000 ppm NaCl–125 ppm SiO_2) with different apparatus of identical single-element (SWC6-MAX) modules which execute either closed- or opened-circuit desalination under fixed pressure (47 bar) of variable flow conditions. The results of this theoretical study reveal milder batch process conditions for CCD compared with OCD manifested by longer sequence duration (23.35 instead of 15.95 min), much lower energy consumption (1.57 instead of 7.93 kWh/m^3) with average TDS of permeates about the same for both processes up to ~75% batch recovery, and higher for the former process (531 instead of 316 ppm TDS) at the ultimate batch recovery of both (~83%) with same pattern also repeated for the average Silica content in permeates (6.76 instead of 3.65 ppm silica). Silica in the recycled concentrates of both CCD and OCD processes is found in the range of 125–728 ± 6 ppm) and reveals desalination under high super-saturation conditions with Silica maximum of ~5.8-fold (~580%) excess over its ordinary saturation level.

Keywords: Reverse osmosis; RO; SWRO; BWRO; Opened-circuit desalination; Closed-circuit desalination; Volume reduction of silica-containing effluents; Rescue and reuse of water from brine effluents

1. Introduction

The declined availability of water in various parts of world due to climate changes inflicted by the global "*green house effect*" combined with the increased contamination of ground and surface water sources have led to the growing reliance on reverse osmosis (RO) desalination processes for seawater and brackish water for domestic supplies. Stringent environmental regulations concerning disposal of industrial and domestic effluents made mandatory in most advanced countries worldwide in order stop the contamination of ground and underground water in parallel to the declined potable water availability, created growing emphasis on advanced technologies for treatment of domestic

and industrial effluents aimed to enable the reuse of rescued treated water.

Treatment of domestic effluents is practiced in gigantic amounts worldwide with treated clean effluents disposed to sea and/or reused for irrigation (e.g. Israel) and/or recycled for domestic use and industrial applications after RO desalination (e.g. Singapore). Complete reclamation of clear domestic effluents in Singapore [1] is practiced currently at the level over 75,000 m^3/d, cover more than 30% of the potable water needs of this country, and the quality of the reclaimed water, or so-called NEWater, is higher than that the other potable water supplies in this country and exceeds the stringent guideline requirements of the both the USEPA and the WHO organizations. NEWater is the brand name given to reclaimed water produced by the Singapore's Public Utilities Board. Instead of exposure to RO for NEWater production, clean domestic effluent could be combined with brine from seawater desalination plants for production of clean hydroelectric power by a membrane-based technology called pressure retarded osmosis [2,3] and this application has been demonstrated by the "Mega-ton" project [4–6] in Japan. In land located brackish water reverse osmosis (BWRO) desalination plants normally face major disposal problems in light of the relatively large amounts of produced brine and in this context, volume reduction techniques on route to zero discharge are of increased importance. In this context, noteworthy is a recent US patent application by Tarquin [7] which describes the further SWRO desalination with recovery >80% of difficult brine effluents (TSD~10,000 ppm and silica >100 ppm) from certain inland BWRO desalination plants which led to increased source utility up to ~96%, and thereby reducing disposal costs.

Treatment of industrial effluents covers broad class processes of increased importance from economic aspects and/or environmental regulations. Industrial effluents are broadly divided into two categories, the first of light effluents mostly in large amounts which can be recycled for reuse with high recovery by simple techniques and the latter of difficult effluents mostly in small amounts which require rigorous treatment before allowed for dumping into municipal sewage systems and/or disposed to the sea and/or rivers. In the case of very hazardous industrial effluents of need to be removed to authorized damping centers, volume reduction techniques are implicated in order to save on transportation costs and dumping expenses.

RO combined with filtration techniques (e.g. MF, UF, and NF) are common features in most effluent treatment processes and the Tarquin process [7] entitle "Sea water RO system to reduce concentrate volume prior to disposal" is noteworthy development which describes

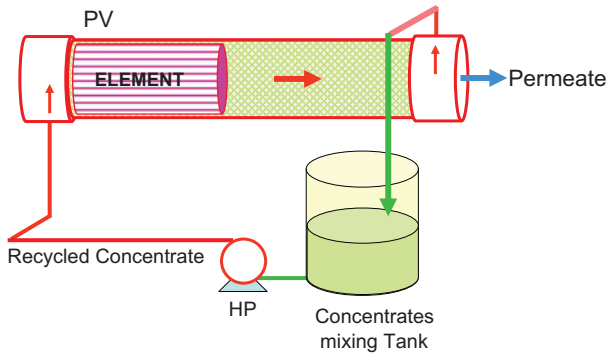

Fig. 1. A schematic design of a single-element PV batch apparatus for an opened-circuit SWRO desalination under fixed pressure (FP) with its HP pump and tank of recycled concentrates—red stands for pressurized sections and green or blue for none pressurized sections in the design.

the application of an Opened Circuit Desalination (OCD) technique which makes use of a single-element module SWRO apparatus of the schematic design in Fig. 1 for 80–85% recovery and thereby, effecting the volume reduction of some very difficult BWRO brine effluents with typical TDS > 10,000 ppm and silica > 125 ppm (e.g. Na, 2,810; K, 113; Ca, 606; Mg, 161; Ba, 0.31; Sr, 17.1; Fe, 0.07; Mn, 0.17; Cl, 5,089; SO4, 1,111; SiO_2, 131; TDS, 10,722 ppm; EC, 18,122 μS/cm; pH, 7.8; turbidity, 0.3 and temperature 25.4°C). This SWRO OCD batch process was carried out under constant applied feed pressure (e.g. 700–740 ψ) of declined flux at low pH (e.g. 3–5) with an effective anti-scaling agent (e.g. Pre-treat Plus-0,400). The application under review demonstrates batch SWRO-OCD under high superconcentration conditions of silica and other constituents (e.g. maximum brine values: TDS > 70,000 ppm; silica > 870 ppm; Ca > 4,000 ppm; Ba > 2.0 ppm and SO_4 > 7,400 ppm) without any noticeable precipitation and therefore, should be found effective for RO treatment of difficult industrial effluents at large. The present theoretical study explores the plausibility of the recently reported [8–11] closed-circuit desalination (CCD) technology (SWRO-CCD) for volume reduction of industrial effluents by analogy with the reported [7] SWRO-OCD batch process.

2. Single-element SWRO-CCD batch apparatus

The schematic design of a single-element SWRO-CCD batch apparatus for volume reduction of effluents under fixed pressure (FP) and variable flow conditions similar to that applied in the opened-circuit process is depicted in Fig. 2. Noteworthy features in the design include the line from module outlet to its

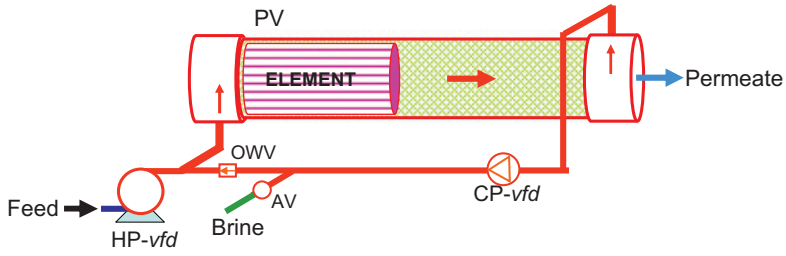

Fig. 2. A schematic design of a single-element apparatus for batch CCD of sea water by reverse osmosis (SWRO-CCD) under FP comprising a PV with a single-element (ELEMENT) inside, a circulation pump with *vfd* (CP-*vfd*), a high-pressure pump with *vfd* (HP-*vfd*), a check valve labeled OWV , an AV, and a manifold connecting the module outlet to its inlet to enable the recycling of concentrates.

inlet and the circulation pump with *vfd* (CP-*vfd*) for concentrate recycling and mixing with fresh pressurized feed at module inlet. The CP-*vfd* enables selected controlled cross-flow over membrane surfaces without which CCD is made impossible due to high-concentration polarization. Pressurized feed in the apparatus under review is created by means of a high-pressure (HP) pump equipped with *vfd* (HP-*vfd*) in order to enable operation under fixed applied pressure of variable flow conditions, or alternatively, under fixed flow of variable pressure conditions, depending of the selected mode of operation. The operation of the unit under FP conditions proceeds with decreased pressurized feed flow of declined permeation flux and when the selected batch sequence recovery manifested by the electric conductivity (EC) of the recycled concentrate is attained, the batch process is stopped, pressure is released, brine inside the apparatus is replaced by fresh feed though the opened actuated valve (AV) at near atmospheric pressure before a new batch sequence initiated. The intent of the check valve labeled one-way-valve (OWV) is to maintain the desired flow direction inside the apparatus.

The batch SWRO-CCD apparatus under review performs with near absolute energy conversion efficiency without ERD irrespective of its operational modes under FP and variable flow or fixed flow and variable pressure conditions. Conversion of this batch apparatus into a configuration for continuous consecutive sequential operation can be achieved by the adding of a side conduit with valve means according to reported [8–11] information elsewhere.

3. Theoretical model performance comparison between single-element SWRO-CCD and SWRO-OCD units under fixed applied pressure conditions

In order to obtain meaningful comparative performance results on the CCD and OCD units, both should be made of the same module design, make use of the same feed source, operate at the same applied pressure, and start operation with the same initial flow rates and module recovery. Both units displayed in Figs. 1 and 2 comprise a single elongated 8-inch pressure vessel with SWC6-MAX element in front and an element spacer next of same intrinsic fluid volume (58.4 L). In both model-simulated processes, the initial flow rates at module inlet (5.45 m^3/h), outlet (3.00 m^3/h), and permeation (2.45 m^3/h) are the same and manifest 45% module recovery at fixed applied pressure of 47 bar for feed of 1.0 NaCl with an osmotic pressure of 8.0 bar. The module inlet flow rate in the CCD process is the sum of the cross-flow (Q_{CP}) and pressurized feed flow (Q_{HP}), whereas in case of the OCD process, the module inlet flow rate is solely that of HP. The selected fixed applied pressure (47 bar) and feed concentration (1.0% NaCl and 125 ppm silica) in the model simulations cover the approximate range reported by Tarquin [7]. The model simulations assume fixed applied pressure (47 bar) of CCD or OCD cycles with progressively declined MR and flux due to the increased salinity of the recycled concentrate with cycle duration (CD) expressing module residence defined from the intrinsic volume of the system and flow rate at module outlet. The CCD and OCD theoretical model simulations on the basis of the aforementioned are described with further details in Tables 1 and 2, respectively.

3.1. Theoretical model batch performance simulation for the SWRO-CCD ME (E = SWC6-MAX) unit with feed of 1.0% NaCl also containing 125 ppm silica under fixed applied pressure of 47 bar

The theoretical model performance simulation of the batch SWRO-CCD unit (Fig. 2) with feed of 1.0% NaCl also containing 125 ppm of Silica under fixed applied pressure of 47 bar with an initial pressurized

feed flow rate of 2.45 m^3/h, initial permeate flow rate of 2.45 m^3/h, fixed flow of recycled concentrates of 3.00 m^3/h, and an initial flow rate at module inlet of 5.45 m^3/h which manifest 45% module recovery is described in Table 1.

The bold data in the table over pale yellow background represent selected features, whereas the rest stands for calculated data. The columns in the table are labeled at the bottom (A1–A30) and the data of each are explained hereinafter. Column A1 identifies the mode (CCD) and the cycle number. Columns A2, A3, and A4 stand for the respective inlet, outlet, and mean module concentrations per given CCD cycle derived from the selected MR for 47 bar applied pressure and the specified flow rates of the HP and CP pumps. Columns A5, A6, and A7 stand for the respective inlet, outlet, and average osmotic pressures per given CCD cycle derived from the appropriate module concentrations. Columns A8, A9, A10, A11, and A12 stand for respective flux and flow rates of HP (Q_{HP}), CP (Q_{CP}), permeate (Q_P), and HP + CP ($Q_{HP} + Q_{CP}$, module inlet) per given CCD cycle with that of CP maintained constant throughout the entire sequence and those of HP and permeate change as function of MR. Columns A13, A14, and A15 stand for the selected MR and calculated *pf* which yield a calculated applied pressure of 47 bar, respectively, with MR defined by Eq. (1) from cited flow rates adjusted per each cycle in compliance with the fixed applied pressure (47 bar) requirements expressed by Eq. (2) and *pf* expressed by Eq. (3), where p_a is applied pressure (bar); μ, flux (lmh); A, permeability coefficient (L/m^2/h/bar); T_{CF}, temperature correction factor; $\Delta\pi_{av}$, average module concentrate-side osmotic pressure (bar); Δp, pressure difference (bar) of CP; p_p, permeate release pressure (bar); π_p, module permeate-side osmotic pressure (bar); Y, MR ratio; and k, an empirical factor determined from the IMS Design data for SWC6-MAX. Columns A16 and A17 stand for CCD CD expressed in min by Eq. (4) and cumulative sequential time (Σmin) expressed by Eq. (5), where Q_{CP} (m^3/h) is cross-flow rate of CP (3.0 m^3/h), V_i, the intrinsic volume of closed circuit (58.4 titer); and N, number of cycles of sequence progression. Noteworthy that CD is maintained fixed (0.75 min/cycle) throughout the sequence since both terms Q_{CP} and V_i remain unchanged. Column A18 stands for permeate volume production at a given cycle [$V_p(N)$-liter] expressed by Eq. (6) and column A19 for the cumulative permeate volume [$\Sigma V(N)$] over the $1 \rightarrow N$ cycles expressed by Eq. (7). Column A20 stands for the mean permeate production (m^3/h) at a given cycle in the sequence derived from $\Sigma V/\Sigma\text{min} \times (60/1{,}000)$ and A21 for the cumulative batch recovery at a given cycle in the progression defined by Eq. (8) on the basis of the cumulative permeate volume (ΣV) and intrinsic closed-circuit volume (V_i).

The power (kW) requirements per cycle in column A22 stand for HP plus CP as defined by the respective expressions Eqs. (9) and (10) with the pertinent parameters of flow rates (m^3/h), pressures (bar), and efficiency ratio of pumps (*f*). The module pressure difference term (Δp) in Eq. (10) is derived from Eq. (11); where $n = 1$ is a single element module; Q_{mi} ($=Q_P + Q_{CP}$), module inlet flow rate; and Q_{mo} ($=Q_{CP}$)—module outlet flow rate. The consumed energy (kWh) per cycle in column A23 is the product of power and CD with cumulative sequential energy (ΣkWh) displayed in column A24 and cumulative specific energy in A25 according to Eq. (12).

The TDS of permeate per cycle in column A26 is derived by Eq. (13), where C_P is permeate TDS; C_f, feed TDS at start of each cycle; and B, the salt diffusion coefficient of the SWC6-MAX element. The TDS of the average permeate during the sequence progression is displayed in column A27 takes into account the accumulation over the preceeding cycles. The concentration (ppm) of silica in permeate per cycle is displayed in column A28 and derived by Eq. (13) from the initial silica concentration per cycle and the relevant *pf* and flux parameters and the average silica concentration during the sequential progression in column A29 is derived by analogy with the average permeate TDS term in column A27. The Silica content in the concentrates (CONC) displayed in column A30 is derived from the initial Silica concentration and the batch recovery terms in column A21.

$$\text{MR}(\%) = 100 \times Q_{HP}/(Q_{HP}+Q_{CP}) = 100 \times Q_P/(Q_P+Q_{CP}) \tag{1}$$

$$p_a = \mu/A/T_{CF} + \Delta\pi_{av} + \Delta p/2 + p_p - \pi_p \tag{2}$$

$$pf = 10^{(k\times Y)} \tag{3}$$

$$\text{CD}\ (\text{minute/cycle}) = (60/1{,}000)\times V_i/Q_{CP} \tag{4}$$

$$\Sigma\text{min} = (60/1{,}000) \times V_i \times N/Q_{CP} \tag{5}$$

$$V_p(N) = [1{,}000/60] \times Q_p(N) \times \text{CD} = Q_p(N) \times V/Q_{CP} \tag{6}$$

$$\Sigma V(N) = V_p(N) + V_p(N-1) + V_p(N-2) + \ldots + V_p(N=1) \tag{7}$$

$$\text{Sequence Recovery} = \Sigma V/(\Sigma V + V_i) \times 100 \quad (8)$$

$$P_{HP}(\text{kW}) = (1/36) \times Q_{HP} \times p_a/f_{HP} = (1/36) \times Q_P \times p_a/f_{HP} \quad (9)$$

$$P_{CP}(\text{kW}) = (1/36) \times Q_{CP} \times \Delta p/f_{CP} \quad (10)$$

$$\Delta p = (8/1,000) \times n \times [(Q_{mi}+Q_{mo})/2]^{1.7} \quad (11)$$

$$\text{Specific Energy } \left(\text{kWh/m}^3\right) = \Sigma kWh/\Sigma V\left(\text{m}^3\right) \quad (12)$$

$$C_p = B \times C_f \times pf \times T_{CF}/\mu \quad (13)$$

3.2. Theoretical model batch performance simulation for the SWRO-OCD ME (E = SWC6-MAX) unit with feed of 1.0% NaCl also containing 125 ppm Silica under fixed applied pressure of 47 bar

The theoretical model performance simulation of the batch SWRO-OCD unit (Fig. 1) with 338 liter feed of 1.0% NaCl also containing 125 ppm silica under fixed applied pressurized (47 bar) conditions with an initial pressurized feed flow rate of 5.45 m^3/h, initial permeate flow rate of 2.46 m^3/h with an initial module recovery of 45% is described in Table 2.

Pressurized feed in the OCD unit design (Fig. 1) is supplied by HP under conditions of fixed flow rate (5.45 m^3/h) at FP (47 bar) though an external Feed Tank containing an initial feed volume of 338 L. Columns B30 and B31 provide the volumetric inventory of feed in the Tank at the start and end of each cycle determined from the released permeate volume per cycle revealed in column B17. The Tank feed concentration (%) at the end of each cycle B32 is estimated from the relevant batch recovery term in column B20 and the end cycle Tank volume in column B31. Accordingly, the module inlet concentration at a given cycle in column B2 is the preceding end-cycle Tank concentration revealed in column B32. The module inlet concentration during the OCD process is determined by the mixing of the brine effluent volume with the leftover volume in the Tank after each cycle, ignoring salt passage to permeates.

In the OCD model data (Table 2), the feed flow rate created by HP is fixed (5.45 m^3/h) with declined permeate flow and flux according to the selected MR required to sustained a fixed applied pressure of 47 bar. The cycle duration (CD) in column B15 is the residence time of the inlet fluid defined from the intrinsic volume of the module (58.4 L) and the flow rate of brine at outlet.

4. Compared performance results of the single element OCD and CCD units

The theoretical model comparison between the FP (47 bar) CCD (Table 1) and OCD (Table 2) batch processes is carried out for units comprising identical modules of same element and intrinsic volume under identical initial conditions of permeate flow rate and MR with model simulation data of declined flux over 20 cycles with 82.65 ± 0.05% batch recovery under fixed operational pressure (47 bar) generated by the same theoretical equations starting with the same feed (1.0% NaCl also containing 125 ppm of silica). The intent of this theoretical study is to explore the performance of both units under super-saturation conditions with respect to silica which according to the reported OCD [7] experiments requires feed pH of 3–5 and an effective anti-scaling agent such as Pre-treat Plus-0400 or alike. In reference to the starting conditions of the batch processes described in Tables 1 and 2, it should be pointed out that running an IMS Design program [12] for a single-element SWC6-MAX [13] module with the same feed (1.0% NaCl also containing 125 ppm of silica) under the specified initial flow conditions of 2.45 m^3/h permeate (60 lmh) with 45% recovery at temperature of 25˚C and pH of 7.0 (instead of 3–5) without the use of an anti-scaling agent led to just one warning statement "concentrate saturation of SiO_2 too high (180%)". Silica scaling restricts the recovery level of many BWRO applications, and the ability to carry out such desalination processes with super-saturated silica concentrates is a subject matter of considerable interest discussed hereinafter in the context of the OCD and CCD batch processes.

The batch progression scales of time, cycles, and recovery for the compared CCD and OCD processes under review are displayed in Fig. 3 and reveal the same number of cycles (20 cycles) of about the same recovery (82.65 ± 0.05%) with sequence periods of 23.35 and 19.94 min, respectively. The longer sequence period duration of the CCD batch is primarily due to the dilution effect whereby recycled concentrates are mixed with fresh pressurized feed at module inlet, thereby, causing lower module inlet concentrations and longer cycles on route to the defined recovery compared with OCD. A longer sequence duration implies a milder pathway of smaller concentration variations and greater uniformity during most of the CCD cycles compared

Table 1
Theoretical model batch performance simulations for the SWRO-CCD ME (E = SWRO-MAX) unit (Fig. 2) with feed of 1.0% NaCl also containing 125 ppm Silica under fixed applied pressure (47 bar) with an initial pressurized feed flow rate of 2.45 m^3/h, initial permeate flow rate of 2.45 m^3/h, fixed flow rate of recycled concentrates of 3.0 m^3/h, initial flow rate at module inlet of 5.45 m^3/h, and initial module recovery of 45.0%

TEST - SWC6 MAX		UNIT DESIGN		OPERATIONAL PARAMETERS	
40.8	m2/Element	1	Modules	1.00	% Feed (NaCl & Silica)
50	m3/day	1	Elements/Module	0.85	Efficiey fator of HP
32,000	ppm NaCl	230	cm long PV	0.70	Efficiey fator of CP
54	bar Applied Pressure	20	cm diameter PV	0.20	bar -Δp CP
10	% Recovery	15	liter element volume	3.00	m3/h CP
25	Centig.	2	% lines volume		
99.50	% Salt Rejection	58.4	liter per module		
28.4	bar NDP			125	ppm Silica in Feed
51.062	l/m2/h Flux	π(bar)-C(%)		1.17	min/cycle
1.798	l/m2/h/bar -A	1.00	ppm TDS Feed		
0.2005	l/m2/h - B	8.00	bar Osmotic Pressure of Feed		
		8.00	π(bar)/C(%)		

CCD	Concentrations			Osmotic Pressures			avarge	Flow Rates				Selected MR & AP		
Cycle	Inlet	outlet	mean	Inlet	outlet	mean	Flux	HP	CP	PERM	HP+CP	MR	*pf*	Calcul.
No	%	%	%	barr	bar	bar	lmh	m3/h	m3/h	m3/h	m3/h	%	factor	bar
1	1.000	1.818	1.409	8.0	14.5	11.3	60.2	2.45	3.00	2.45	5.45	**45.0**	1.199	47.0
2	1.484	2.507	1.996	11.9	20.1	16.0	50.7	2.07	3.00	2.07	5.07	**40.8**	1.179	47.0
3	1.956	3.085	2.520	15.6	24.7	20.2	42.4	1.73	3.00	1.73	4.73	**36.6**	1.159	47.0
4	2.405	3.568	2.987	19.2	28.5	23.9	35.6	1.45	3.00	1.45	4.45	**32.6**	1.140	47.0
5	2.831	3.971	3.401	22.6	31.8	27.2	29.6	1.21	3.00	1.21	4.21	**28.7**	1.123	47.0
6	3.228	4.304	3.766	25.8	34.4	30.1	24.5	1.00	3.00	1.00	4.00	**25.0**	1.106	47.0
7	3.587	4.581	4.084	28.7	36.7	32.7	20.4	0.83	3.00	0.83	3.83	**21.7**	1.091	47.0
8	3.915	4.810	4.363	31.3	38.5	34.9	16.8	0.69	3.00	0.69	3.69	**18.6**	1.078	47.0
9	4.200	5.000	4.600	33.6	40.0	36.8	14.0	0.57	3.00	0.57	3.57	**16.0**	1.067	47.0
10	4.460	5.156	4.808	35.7	41.3	38.5	11.5	0.47	3.00	0.47	3.47	**13.5**	1.056	47.0
11	4.683	5.285	4.984	37.5	42.3	39.9	9.5	0.39	3.00	0.39	3.39	**11.4**	1.047	47.0
12	4.874	5.391	5.132	39.0	43.1	41.1	7.8	0.32	3.00	0.32	3.32	**9.6**	1.039	47.0
13	5.040	5.478	5.259	40.3	43.8	42.1	6.4	0.26	3.00	0.26	3.26	**8.0**	1.033	47.0
14	5.178	5.550	5.364	41.4	44.4	42.9	5.3	0.22	3.00	0.22	3.22	**6.7**	1.027	47.0
15	5.295	5.609	5.452	42.4	44.9	43.6	4.4	0.18	3.00	0.18	3.18	**5.6**	1.023	47.0
16	5.397	5.658	5.527	43.2	45.3	44.2	3.5	0.14	3.00	0.14	3.14	**4.6**	1.019	47.0
17	5.485	5.696	5.591	43.9	45.6	44.7	2.8	0.12	3.00	0.12	3.12	**3.7**	1.015	47.0
18	5.546	5.729	5.637	44.4	45.8	45.1	2.4	0.10	3.00	0.10	3.10	**3.2**	1.013	47.0
19	5.606	5.756	5.681	44.8	46.0	45.4	2.0	0.08	3.00	0.08	3.08	**2.6**	1.011	47.0
20	5.661	5.776	5.718	45.3	46.2	45.7	1.5	0.06	3.00	0.06	3.06	**2.0**	1.008	47.0
A1	**A2**	**A3**	**A4**	**A5**	**A6**	**A7**	**A8**	**A9**	**A10**	**A11**	**A12**	**A13**	**A14**	**A15**

Table 1 continued

CCD	Batch Duration & Permeates Volunes						HP+CP: Power & Energy				Permeate TDS		Permeate Silica		CONC.
Cycle	Cycle	Total	Cycle	ΣV	mean	Batch	per Cycle		per Batch		Cycle	average	Cycle	average	Silica
No	min	Σmin	liter	liter	m3/h	%	kW	kWh	ΣkWh	kWh/m3	ppm	ppm	ppm	ppm	ppm
1	1.17	1.17	47.8	47.8	2.45	45.0	3.792	0.0738	0.074	1.545	56	56	0.50	0.50	227
2	1.17	2.33	40.2	88.0	2.26	60.1	3.200	0.0623	0.136	1.546	93	73	1.06	0.76	313
3	1.17	3.50	33.7	121.7	2.08	67.6	2.682	0.0522	0.188	1.547	138	91	1.72	1.02	386
4	1.17	4.67	28.2	149.9	1.93	72.0	2.254	0.0438	0.232	1.548	192	110	2.48	1.30	446
5	1.17	5.84	23.5	173.4	1.78	74.8	1.879	0.0366	0.269	1.549	259	130	3.39	1.58	496
6	1.17	7.00	19.5	192.8	1.65	76.8	1.558	0.0303	0.299	1.550	341	151	4.49	1.87	538
7	1.17	8.17	16.2	209.0	1.53	78.2	1.301	0.0253	0.324	1.551	439	174	5.78	2.18	573
8	1.17	9.34	13.3	222.4	1.43	79.2	1.076	0.0209	0.345	1.552	561	197	7.36	2.49	601
9	1.17	10.51	11.1	233.5	1.33	80.0	0.902	0.0176	0.363	1.554	702	221	9.18	2.81	625
10	1.17	11.67	9.1	242.6	1.25	80.6	0.743	0.0145	0.377	1.555	887	246	11.53	3.13	645
11	1.17	12.84	7.5	250.1	1.17	81.1	0.617	0.0120	0.389	1.556	1,106	272	14.30	3.47	661
12	1.17	14.01	6.2	256.3	1.10	81.5	0.513	0.0100	0.399	1.557	1,370	298	17.63	3.81	674
13	1.17	15.17	5.1	261.4	1.03	81.7	0.425	0.0083	0.407	1.559	1,703	326	21.82	4.16	685
14	1.17	16.34	4.2	265.6	0.98	82.0	0.355	0.0069	0.414	1.560	2,092	353	26.71	4.52	694
15	1.17	17.51	3.5	269.0	0.92	82.2	0.297	0.0058	0.420	1.562	2,563	382	32.61	4.88	701
16	1.17	18.68	2.8	271.8	0.87	82.3	0.246	0.0048	0.425	1.563	3,184	411	40.39	5.25	707
17	1.17	19.84	2.2	274.1	0.83	82.4	0.201	0.0039	0.429	1.564	4,027	441	50.94	5.62	712
18	1.17	21.01	1.9	276.0	0.79	82.5	0.176	0.0034	0.432	1.566	4,710	470	59.49	6.00	716
19	1.17	22.18	1.6	277.6	0.75	82.6	0.147	0.0029	0.435	1.567	5,864	501	73.92	6.38	719
20	1.17	23.35	1.2	278.8	0.72	82.7	0.118	0.0023	0.437	1.569	7,702	531	96.90	6.76	722
A1	**A16**	**A17**	**A18**	**A19**	**A20**	**A21**	**A22**	**A23**	**A24**	**A25**	**A26**	**A27**	**A28**	**A29**	**A30**

with those of OCD as evident by the inlet–outlet module concentration variations on the recovery scale revealed in Fig. 4; wherein CCD concentrations are shown to remain significantly below those of OCD and reach the same proximity only towards the end of batch recovery sequences. The Tank feed volume changes during the OCD batch process are displayed in Fig. 5 as a function of cycles (A), sequence time progression (B), and recovery (C). Likewise, the Tank feed concentration variations are displayed in Fig. 6 as a function of cycles (A), sequence time progression (B), and recovery (C), respectively.

Osmotic pressures' variations at module inlet–outlet during the CCD and OCD batch processes under review due to change of concentrations (Fig. 4) are displayed in Fig. 7 as a function of recovery with reference to the fixed applied pressure. In these batch processes, both inlet and outlet concentrations and osmotic pressures increase simultaneously as function of batch sequence progression along the time, cycles, and recovery scales and this implies declined net driving pressure (NDP = $p_a - \Delta\pi$), or declined flux, since applied pressure (p_a) is maintained constant. Batch processes under fixed applied pressure such as CCD and OCD are characterized by declined flux, MR, and concentration polarization factor and these features in the context of the current study are revealed on the recovery scale in Fig. 8(A, B, and C), respectively. Permeate production variations per cycle and average on the recovery scale of the compared CCD (Table 1) and OCD (Table 2) batch processes in Fig. 9 reveal an average of 0.72 m^3/h after 23.3 min of 278.8 L permeate volume received with 82.7% recovery by the former and 1.06 m^3/h after 15.94 min of 280.4 L permeate volume received with 82.9% recovery by the later. Both processes start with same CD (1.17 min/cycle) and permeate production rate (2.45 m^3/h); however, the CD during OCD declines (1.17—0.64 min/cycle), whereas that of CCD remains constant and this implies more early batch cycles of greater contribution to the average permeate production in the OCD process as is manifested by the comparative results in Fig. 9. The compared batch production rates derived from $\Sigma V/\Sigma$min manifest similar ΣV terms (278.8 and 280.4 L) and a much shorter Σmin for OCD (15.9 vs. 23.3 min) for reasons already discussed.

Permeate TDS variations of the compared CCD (Table 1) and OCD (Table 2) batch processes in Fig. 10 reveal higher per cycle values for latter with a similar average up to 75% recovery and thereafter, a higher average for the former. The compared values per cycle are consistent with the faster declined flux, MR, and concentration polarization of the OCD batch process displayed in Fig. 8(A, B, and C), respectively. In contrast with TDS values per cycle, the average TDS incorporates contributions of preceeding cycles and passing the ~75% recovery level with CCD requires additional 15 cycles of 17.51 min duration for 105.5 L permeate production in order to complete the batch recovery of 82.4%; whereas in case of OCD, the need is of additional 12 cycles of 8.04 min duration for 29.5 L permeate production in order to reach a similar recovery level. The fewer number of cycles of diminished duration for a smaller permeate volume production in case of the OCD batch process compared with CCD dictates the improved average TDS of permeates observed for the former process. Silica TDS values in permeates (Fig. 11) and concentrates (Fig. 12) of the compared CCD (Table 1) and OCD (Table 2) batch processes are noteworthy since both processes are performed with silica-saturated feed and silica supersaturated concentrates at low pH in the presence of an appropriate antiscalant under which conditions supersaturation with respect to silica was claimed [7] to be undisrupted. The Silica pattern in permeates displayed in Fig. 11 is exactly analogous to that of TDS in Fig. 10 for the same reasons already discussed. The maximum permeate Silica per cycle at the last batch cycle (number 20) is 96.9 ppm for CCD (Table 1) and 1,100 ppm for OCD (Table 2) manifesting the shorter cycles (0.64 instead 1.17 min/cycle) of lower permeate volume production (0.06 instead of 1.2 L) by the latter. In simple terms, the OCD batch process creates permeates of exceptionally high Silica content with increased recovery and such an effect with CCD takes place in a milder form. The super-saturation of silica in the recycled concentrates of the batch processes under review is evident in Fig. 12 with identical rise of Silica super-saturation as a function of increased recovery. Silica of 125 ppm in the feed of the simulated processes corresponds to the saturation limit of 100% and therefore right from start, the Silica content in recycled concentrates of said processes exceeds the saturation level with increased super-saturation concomitant with increased recovery. Silica concentrations at the end of the compared processes (SiO_2: 722–734 ppm) exceed the saturation limits by ~5.8-fold (580%) and the ability to desalinate under such extraordinarily high super-saturation level most obviously relates to the reported [7] conditions of a declined flux batch process at low pH in the presence of effective scaling inhibitors with demonstrated maximum silica super-saturation exceeding 1,000 ppm.

Specific energy (SE) variations as function of recovery of the compared CCD (Table 1) and OCD (Table 2) batch processes are displayed in Fig. 13. The SE_{CCD} of CCD during the batch sequence progression originates from the HP and the CP pumps according to Eqs. (14)

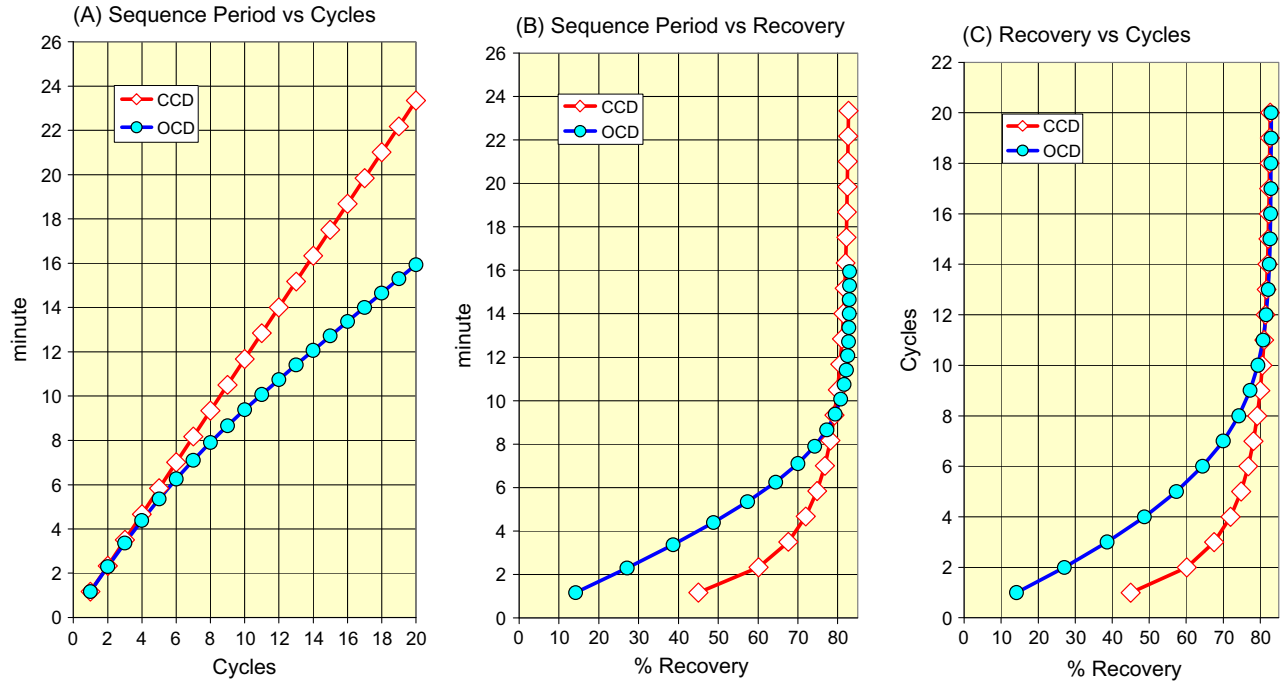

Fig. 3. Batch sequence period vs. cycles (A) and recovery (B) as well as cycles vs. recovery (C) for the compared CCD (Table 1) and OCD (Table 2) batch processes under FP of declined flux.

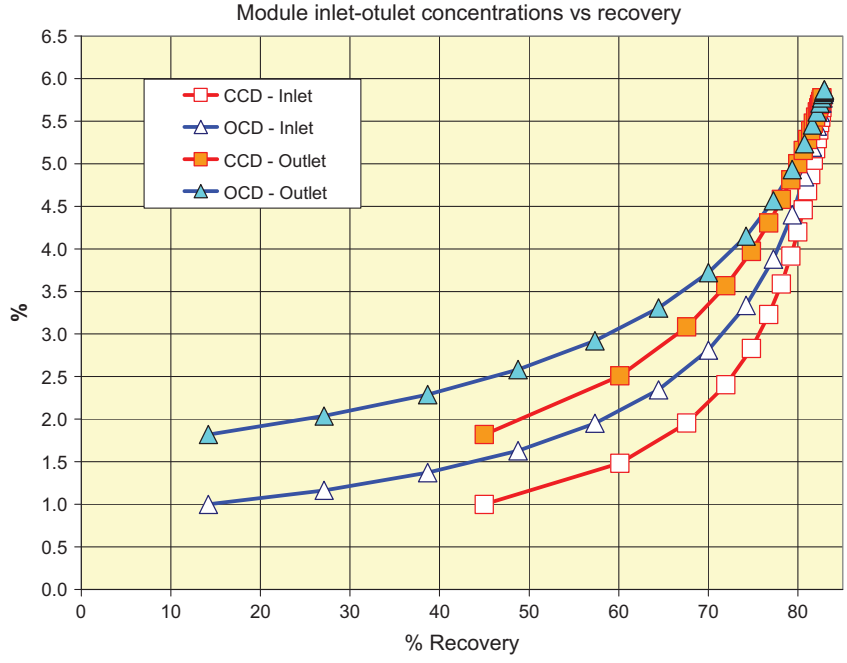

Fig. 4. Batch sequence variations of module inlet–outlet concentrations as function of recovery for the compared CCD (Table 1) and OCD (Table 2) batch processes under FP of declined flux.

and (15), respectively. The flow rate of HP and permeate in CCD are the same, and this implies according to Eq. (14) on the basis of the data in Table 1 fixed $SE_{HP\text{-}CCD}$ of 1.536 kWh/m^3. The $SE_{CP\text{-}CCD}$ according to Eq. (15) is a function of the cited flow rates which manifest the range of 0.0097–0.396 kWh/m^3 and an average of

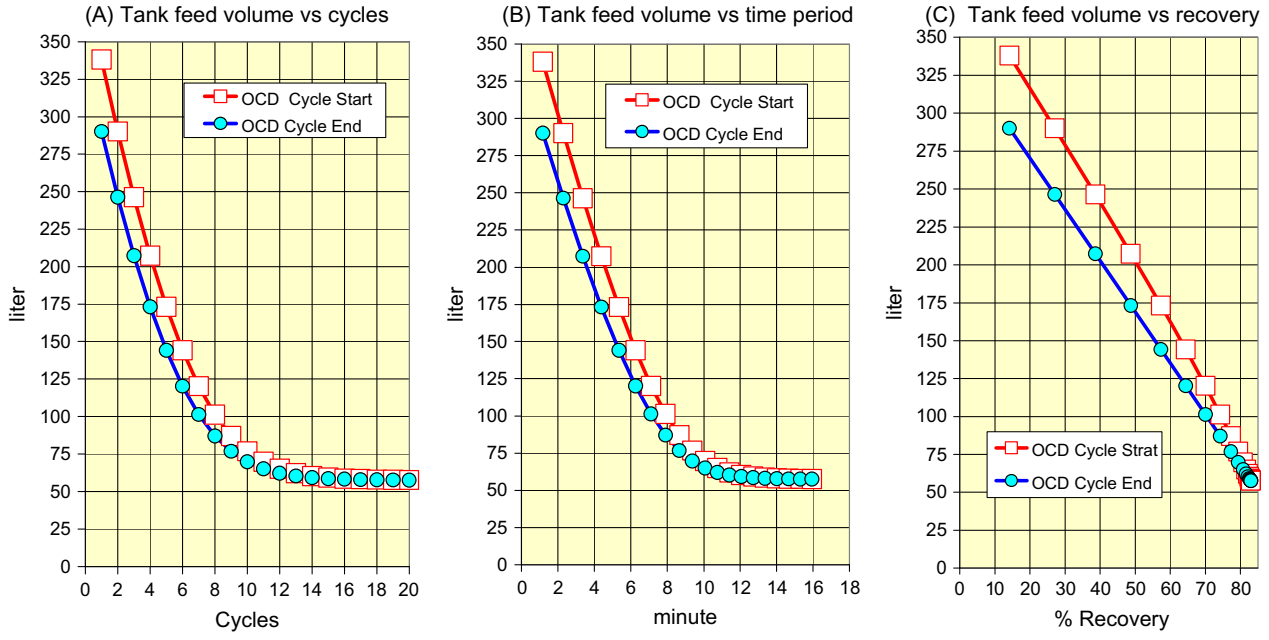

Fig. 5. Tank feed volume variations during the OCD batch process as function of cycles (A), batch sequence duration (B), and recovery (C) according to the data in Table 2.

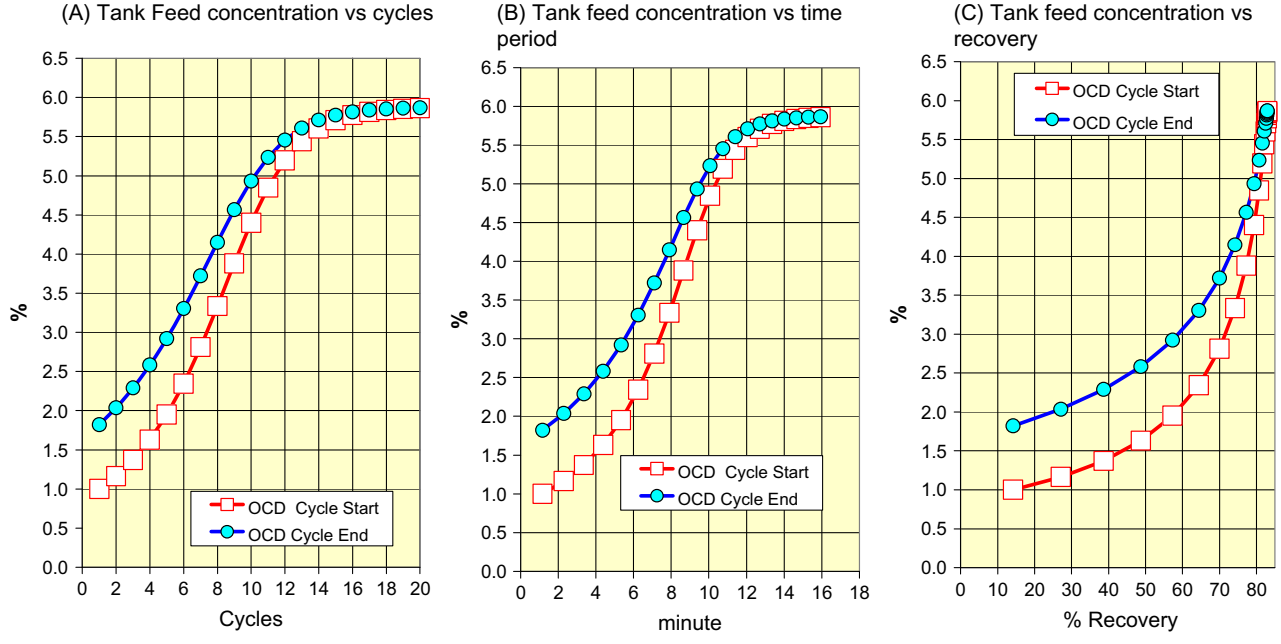

Fig. 6. Tank feed concentration variations during the batch OCD process as function of cycles (A), batch sequence duration (B), and recovery (C) according to the data in Table 2.

0.203 kWh/m^3 for the entire batch sequence. The aforementioned explains the small SE_{CCD} variability (1.545–1.569 kWh/m^3) revealed in Fig. 13 for the CCD process. The power consumption of HP during the OCD according the data in Table 2 is fixed (8.4 kW); however, $SE_{HP\text{-}OCD}$ is also a function of the declined flow rate of the permeate [Eq. (16)] with average increases in the range 3.409–7.930 kWh/m^3 from start

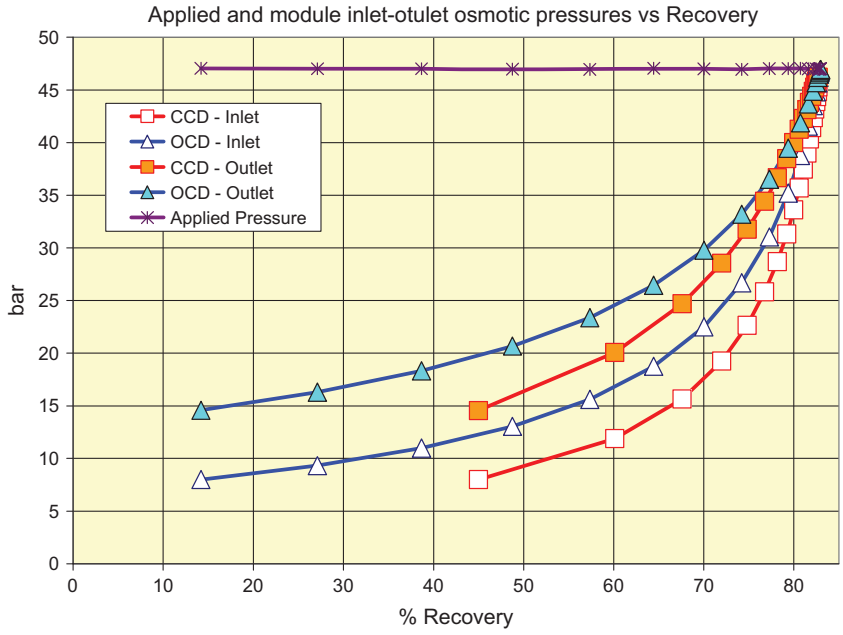

Fig. 7. Batch sequence variations of module inlet–outlet osmotic pressures as function of recovery for the compared CCD (Table 1) and OCD (Table 2) batch processes under FP of declined flux.

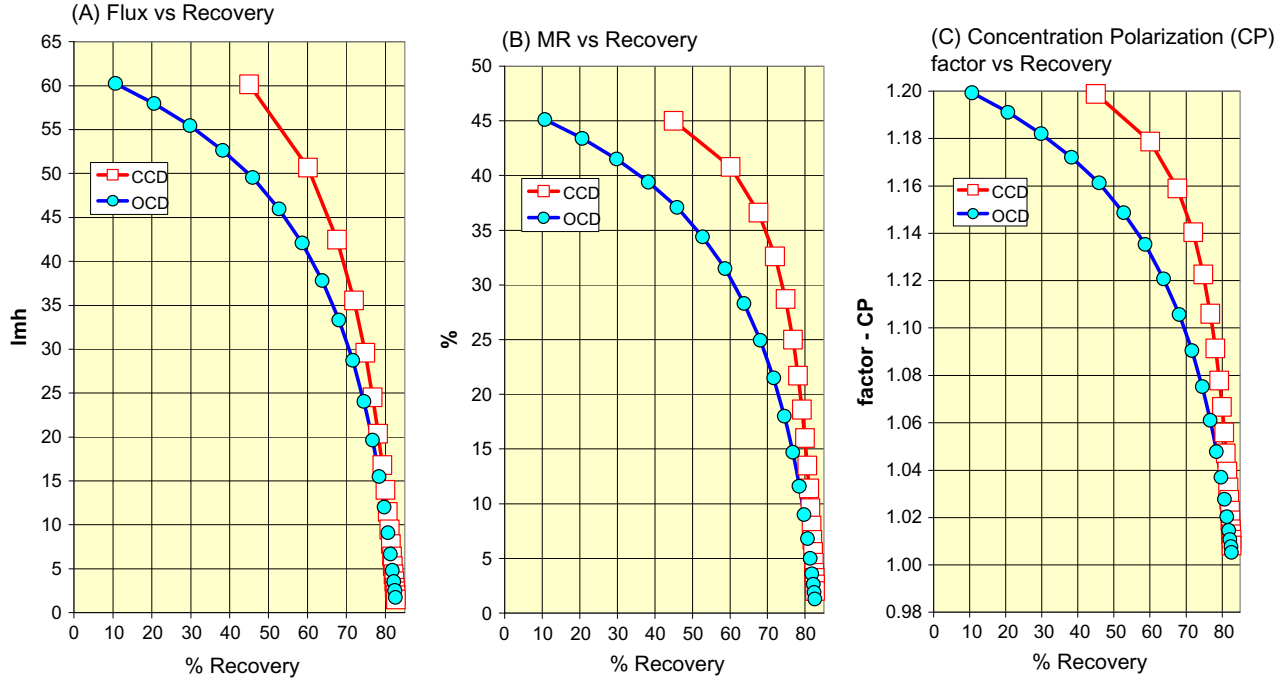

Fig. 8. Batch sequence variations of flux (A), MR (B), and concentration polarization factor (C) as function of recovery for the compared CCD (Table 1) and OCD (Table 2) batch processes under fixed applied pressure of declined flux.

to end of this batch sequence. The $SE_{HP\text{-}OCD}$ per cycle during this OCD process corresponds to an extraordinarily large range starting at 3.409 kWh/m^3 and climbing exponentially to 840 kWh/m^3 (8.40/0.01) at the end of the OCD batch process where Q_p = 0.01 m^3/h. The data in Tables 1 and 2 reveal energy saving by

Table 2
Theoretical model batch performance simulations for the SWRO-OCD ME (*E* = SWRO-MAX) unit (Fig. 1) with 338 liter feed of 1.0% NaCl also containing 125 ppm silica under fixed applied pressure (47 bar) with an initial pressurized feed flow of 5.45 m^3/h, initial permeate flow of 2.46 m^3/h, and initial module recovery of 45.1%

TEST - SWC6 MAX		UNIT DESIGN		OPERATIONAL PARAMETERS	
40.8	m2/Element	1	Modules	1.00	% Feed (NaCl & Silica)
50	m3/day	1	Elements/Module	0.85	Efficiey fator of HP
32,000	ppm NaCl	230	cm long PV	0.70	Efficiey fator of CP
54	bar Applied Pressure	20	cm diameter PV	5.45	m3/h fixed feed inlet
10	% Recovery	15	liter element volume		
25	Centig.	2	% lines volume	338	liter - Tank
99.50	% Salt Rejection	58.4	liter per module	125	ppm Silica
28.4	bar NDP				
51.062	l/m2/h Flux	π(bar)-C(%)			
1.798	l/m2/h/bar -A	1.00	ppm TDS Feed		
0.2005	l/m2/h - B	8.00	bar Osmotic Pressure of Feed		
		8.00	π(bar)/C(%)		

OCD	Concentrations			Osmotic Pressures			av.	Flow Rates			Selected MR & AP		
Cycle	Inlet	outlet	mean	Inlet	outlet	mean	Flux	HP	Brine	PERM	MR	*pf*	Calcul.
No	%	%	%	barr	bar	bar	lmh	m3/h	m3/h	m3/h	%	factor	bar
1	1.000	1.821	1.411	8.0	14.6	11.3	60.2	5.45	2.99	2.46	**45.10**	1.199	47.0
2	1.165	2.037	1.601	9.3	16.3	12.8	57.2	5.45	3.12	2.33	**42.80**	1.188	47.0
3	1.372	2.290	1.831	11.0	18.3	14.6	53.6	5.45	3.26	2.19	**40.10**	1.175	47.0
4	1.630	2.584	2.107	13.0	20.7	16.9	49.3	5.45	3.44	2.01	**36.90**	1.160	47.0
5	1.952	2.922	2.437	15.6	23.4	19.5	44.3	5.45	3.64	1.81	**33.20**	1.143	47.0
6	2.344	3.307	2.826	18.8	26.5	22.6	38.9	5.45	3.86	1.59	**29.10**	1.124	47.0
7	2.812	3.721	3.267	22.5	29.8	26.1	32.7	5.45	4.12	1.33	**24.45**	1.104	47.0
8	3.336	4.149	3.742	26.7	33.2	29.9	26.2	5.45	4.38	1.07	**19.60**	1.082	47.0
9	3.881	4.565	4.223	31.0	36.5	33.8	20.0	5.45	4.63	0.82	**15.00**	1.062	47.0
10	4.401	4.934	4.667	35.2	39.5	37.3	14.4	5.45	4.86	0.59	**10.80**	1.044	47.0
11	4.847	5.234	5.041	38.8	41.9	40.3	9.9	5.45	5.05	0.40	**7.40**	1.030	47.0
12	5.19	5.46	5.33	41.6	43.6	42.6	6.4	5.45	5.19	0.26	**4.80**	1.020	47.0
13	5.44	5.61	5.52	44	44.9	44.2	4.0	5.45	5.29	0.16	**3.00**	1.012	47.0
14	5.60	5.71	5.66	45	45.7	45.3	2.5	5.45	5.35	0.10	**1.90**	1.008	47.0
15	5.71	5.77	5.74	46	46.2	45.9	1.5	5.45	5.39	0.06	**1.10**	1.004	47.0
16	5.77	5.81	5.79	46	46.5	46.4	0.9	5.45	5.41	0.04	**0.70**	1.003	47.0
17	5.81	5.84	5.83	47	46.7	46.6	0.5	5.45	5.43	0.02	**0.40**	1.002	47.0
18	5.84	5.85	5.85	47	46.8	46.8	0.3	5.45	5.44	0.01	**0.25**	1.001	47.0
19	5.85	5.86	5.9	47	46.9	46.9	0.2	5.45	5.44	0.01	**0.18**	1.001	47.0
20	5.86	5.87	5.9	47	47.0	46.9	0.1	5.45	5.44	0.01	**0.10**	1.000	47.0
B1	**B2**	**B3**	**B4**	**B5**	**B6**	**B7**	**B8**	**B9**	**B10**	**B11**	**B12**	**B13**	**B14**

Table 2 continued

OCD	Batch Duration & Permeate Volume						HP Power & Energy				Permeate TDS		Permeate Silica		CONC.	Tank Balance		
Cycle	Cycle	Total	Cycle	ΣV	mean	Batch	per Cycle		per Batch		Cycle	av	Cycle	av	Silica	start	End	End
No	min	Σmin	liter	liter	m3/h	%	kW	kWh	ΣkWh	kWh/m3	ppm	ppm	ppm	ppm	ppm	liter	ltier	%
1	1.17	1.17	47.9	47.9	2.46	14.19	8.4	0.1634	0.163	3.409	56	56	0.50	0.50	146	338.0	290.1	1.165
2	1.12	2.29	43.7	91.6	2.40	27.11	8.4	0.1568	0.320	3.495	67	61	0.61	0.55	171	290.1	246.4	1.372
3	1.07	3.37	39.1	130.7	2.33	38.67	8.4	0.1497	0.470	3.596	81	67	0.75	0.61	204	246.4	207.3	1.630
4	1.02	4.38	34.1	164.8	2.26	48.76	8.4	0.1420	0.612	3.713	99	74	0.96	0.68	244	207.3	173.2	1.952
5	0.96	5.35	29.0	193.8	2.18	57.35	8.4	0.1341	0.746	3.849	126	82	1.26	0.77	293	173.2	144.2	2.344
6	0.91	6.25	24.0	217.8	2.09	64.43	8.4	0.1265	0.872	4.006	164	91	1.70	0.87	351	144.2	120.2	2.812
7	0.85	7.10	18.9	236.7	2.00	70.02	8.4	0.1187	0.991	4.188	221	101	2.38	0.99	417	120.2	101.3	3.336
8	0.80	7.90	14.2	250.9	1.90	74.23	8.4	0.1114	1.103	4.394	310	113	3.46	1.13	485	101.3	87.1	3.881
9	0.76	8.66	10.3	261.2	1.81	77.28	8.4	0.1055	1.208	4.625	449	126	5.16	1.29	550	87.1	76.8	4.401
10	0.72	9.38	7.1	268.3	1.72	79.37	8.4	0.1005	1.309	4.878	677	141	7.98	1.47	606	76.8	69.7	4.847
11	0.69	10.07	4.7	272.9	1.63	80.75	8.4	0.0969	1.406	5.150	1,053	156	12.66	1.66	649	69.7	65.1	5.194
12	0.67	10.75	2.94	275.9	1.54	81.62	8.4	0.0942	1.500	5.436	1,698	173	20.70	1.86	680	65.1	62.1	5.440
13	0.66	11.41	1.81	277.7	1.46	82.15	8.4	0.0923	1.592	5.733	2,797	190	34.43	2.07	700	62.1	60.3	5.603
14	0.65	12.07	1.13	278.8	1.39	82.49	8.4	0.0914	1.683	6.038	4,503	207	55.75	2.29	714	60.3	59.2	5.710
15	0.65	12.71	0.65	279.5	1.32	82.68	8.4	0.0906	1.774	6.348	7,869	225	97.82	2.51	722	59.2	58.5	5.773
16	0.65	13.36	0.41	279.9	1.26	82.80	8.4	0.0903	1.864	6.661	12,457	243	155.17	2.74	727	58.5	58.1	5.814
17	0.65	14.01	0.23	280.1	1.20	82.87	8.4	0.0900	1.954	6.977	21,895	261	273.14	2.96	730	58.1	57.9	5.838
18	0.64	14.65	0.15	280.2	1.15	82.91	8.4	0.0899	2.044	7.294	35,126	279	438.52	3.19	732	57.9	57.8	5.853
19	0.64	15.29	0.11	280.4	1.10	82.94	8.4	0.0899	2.134	7.612	48,879	298	610.43	3.42	733	57.8	57.6	5.863
20	0.64	15.94	0.06	280.4	1.06	82.96	8.4	0.0898	2.224	7.930	88,078	316	1100.43	3.65	734	57.6	57.6	5.869
B1	**B15**	**B16**	**B17**	**B18**	**B19**	**B20**	**B21**	**B22**	**B23**	**B24**	**B25**	**B26**	**B27**	**B28**	**B29**	**B30**	**B31**	**B32**

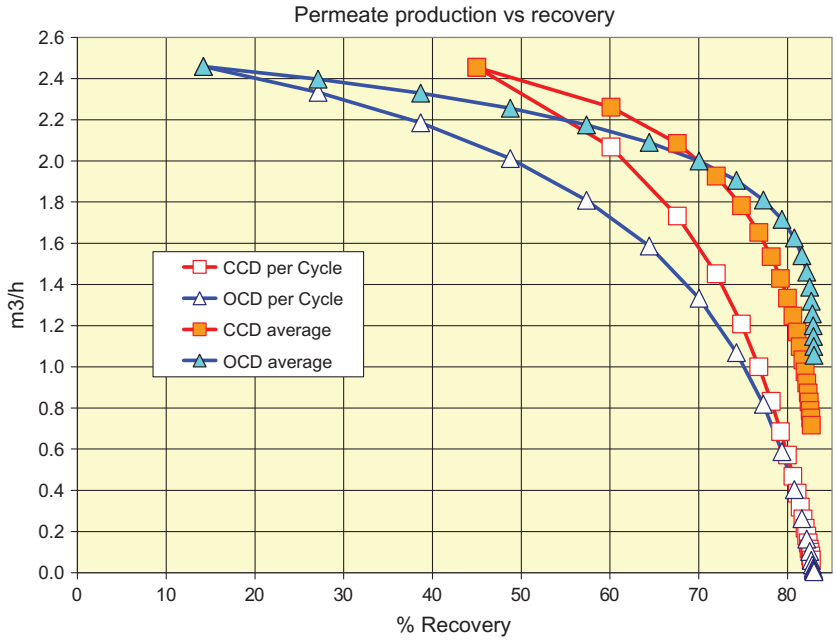

Fig. 9. Permeate production rate variations per cycle and average as function of recovery for the compared CCD (Table 1) and OCD (Table 2) batch processes under fixed applied pressure of declined flux.

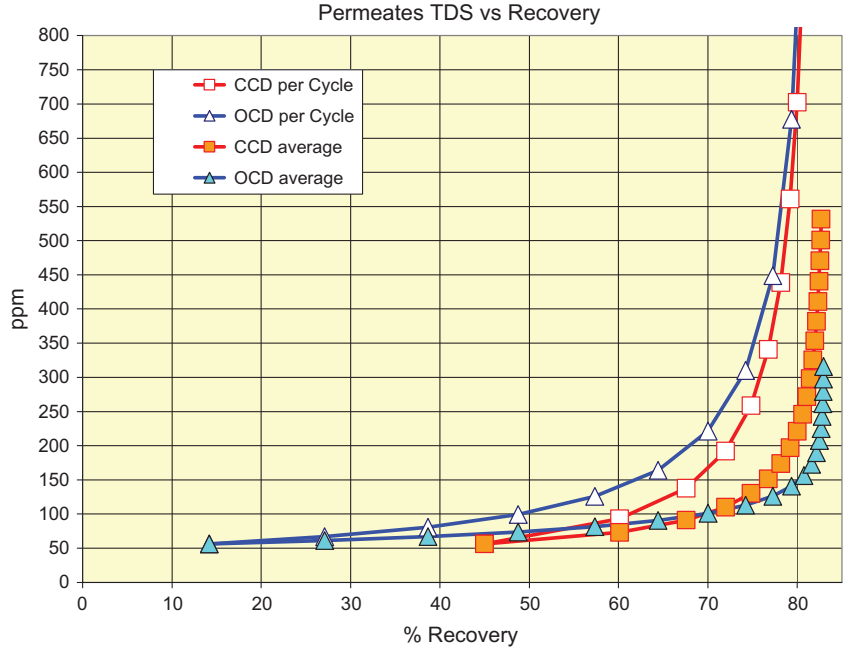

Fig. 10. Permeates TDS variations as function of recovery for the compared CCD (Table 1) and OCD (Table 2) processes under fixed applied pressure of declined flux.

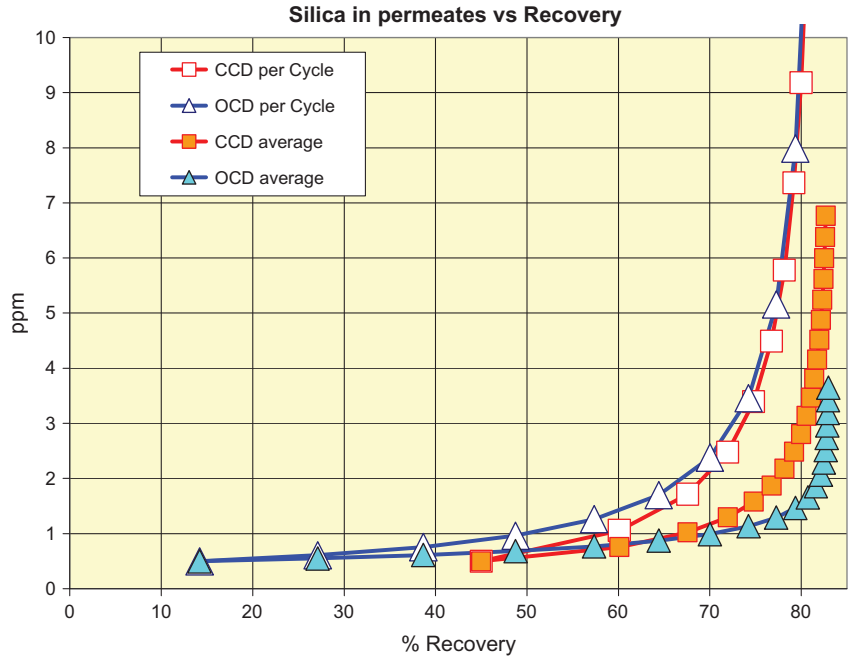

Fig. 11. Silica content in permeates as function of recovery for the compared CCD (Table 1) and OCD (Table 2) processes under fixed applied pressure of declined flux.

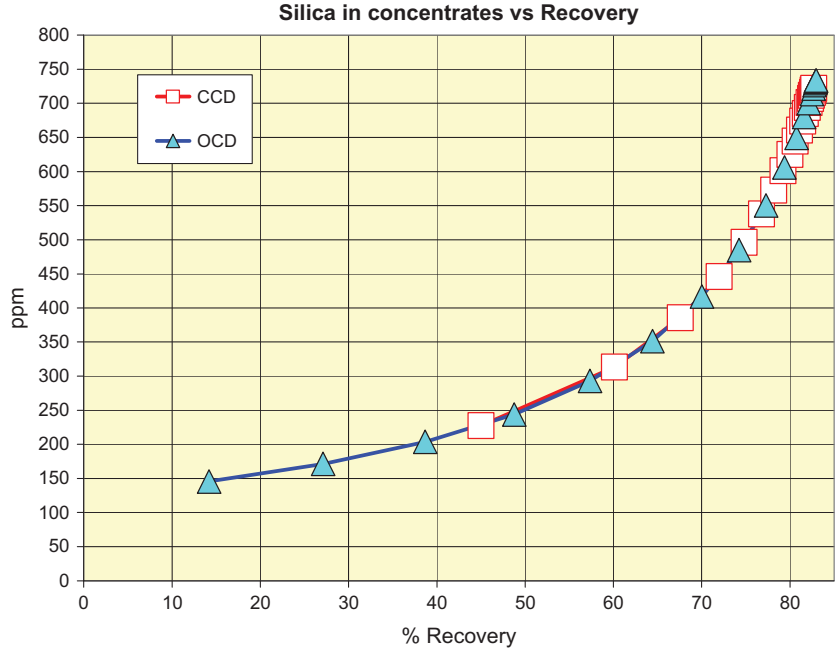

Fig. 12. Silica content in recycled concentrates as function of recovery in the compared CCD (Table 1) and OCD (Table 2) processes under fixed applied pressure of declined flux.

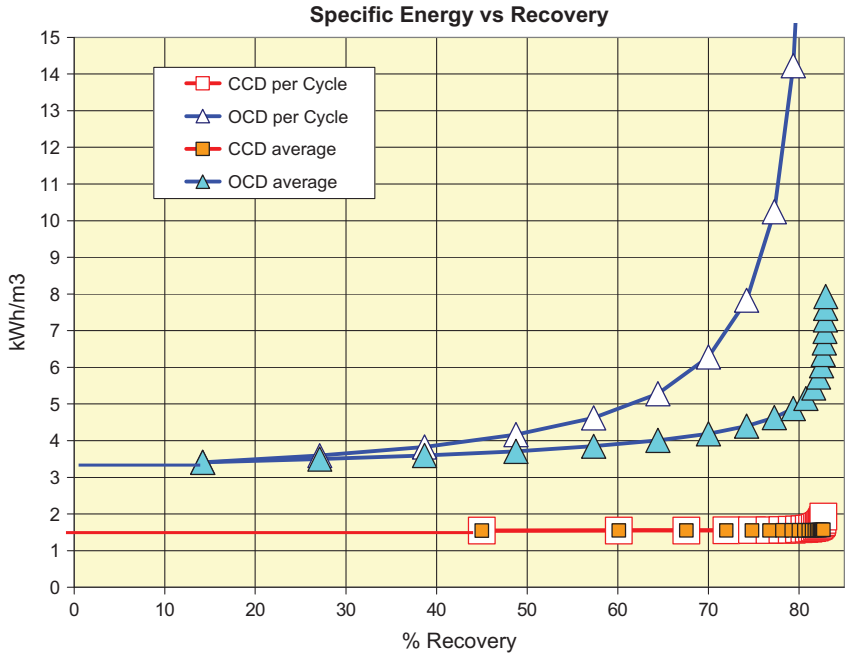

Fig. 13. Specific energy as function of recovery in the compared CCD (Table 1) and OCD (Table 2) processes under fixed applied pressure of declined flux.

CCD compared with OCD as a function of recovery (R) of 62.9% at $R = 70.\%$, 68.1% at $R = 80.8\%$, and 80.2% at $R = 82.9\%$.

$$SE_{HP-CCD} = P_{HP}(kW)/Q_P(m^3/h) = (1/36) \times (Q_{HP}/Q_P) \times p_a/f_{HP} = (1/36) \times p_a/f_{HP} \quad (14)$$

$$SE_{CP-CCD} = P_{CP}(kW)/Q_P(m^3/h) = (1/36) \times (Q_{CP}/Q_P) \times \Delta p/f_{CP} \quad (15)$$

$$SE_{HP-OCD} = P_{HP}(kW)/Q_P(m^3/h) = (1/36) \times (Q_{HP}/Q_P) \times p_a/f_{HP} \quad (16)$$

5. Discussion

The noteworthy results of volume reduction and water rescue from BWRO brine effluents of high Silica content reported [7] with single-element module for SWRO-OCD apparatus most probably manifest the conditions the trials at low pH in the presence of effective antisclant for Silica under declined flux of a batch process with an effective control of the membrane performance made possible by single-element modules. The comparative theoretical model performance analysis of the same feed source using identical single-element modules under same initial flow rates, MR, and ultimate recovery conditions in the context of SWRO-OCD and SWRO-CCD reveals a milder process of much lower energy consumption (Fig. 13) for the latter process with similar average TDS of permeates (Fig. 10) and Silica content (Fig. 11) of same Silica content in both brine effluents (Fig. 12). The dilution effect only possible with the CCD process further reduces the probability of scaling. The entire process in CCD is carried out in the closed circuit without need for an external Tank and thereby, avoiding contact between the recycled concentrates and air which in some cases may cause undesirable oxidation of certain brine components if found (e.g. H_2S). In light of the aforementioned, it would appear that CCD should be preferred over OCD for volume reduction of brine effluents at large.

A reference [7] in the context of batch SWRO-OCD suggested the possibility of similar volume reduction processes also with modules containing more than one element and the same also applies to the SWRO-CCD facility in light of its dilution effect. The CCD process enables considerable module performance flexibility and versatility not possible with OCD such as an initial batch process under fixed flow and variable pressure conditions with fixed flux and low MR (<15%) and *on-line* change of operational mode at a selected applied pressure set point to FP of variable flow

condition until the ultimate desired recovery is attained. A duel operational modes batch CCD should enable even milder conditions of volume reduction with lower energy requirement and reasonable permeates of low silica content, since the declined volumes of high TDS contributes meaningfully to the average TDS of permeates only towards the end of the batch process.

In the reported [7] OCD process, emphasis was made to the restored membrane performance after each batch sequence by brief rinse with permeate and this also explained the preference of a batch-style process for such an application. The broader aspects of desalination under super-saturation Silica conditions are of general interest also for continuous BWRO desalination processes of high Silica feed of confined recovery prospects and no simple means to restore membrane performance by rinsing with permeate as in case of batch processes. While this subject matter is beyond the immediate scope of the current study on volume reduction of difficult Silica-containing effluents, it should be noteworthy that preliminary results [14] on continuous BWRO-CCD desalination of a domestic water sources in Israel with 78 ppm nitrate and 37 ppm silica at ordinary pH 7.0 using modules of three elements and antisacalants revealed the attainment of 88%–93% recovery under continuous operational conditions with the respective brine Silica range of 308–528 ppm, well above the ordinary saturation level of Silica. The aforementioned may suggest that both batch and continuous CCD processes are of lower scaling characteristics compared with conventional PFD techniques and may be used effectively to enhance BWRO recovery of high silica-containing sources.

6. Summary

In light of the recent demonstration of brine (>10,000 ppm TDS with silica >124 ppm) volume reduction by an OCD of 80–85% recovery using SWRO batch apparatus containing single-element modules operated at low pH with fixed applied pressure of declined flux under high super-saturation conditions with respect to silica, the present study assesses an analogous process under CCD conditions. In order to compare between the OCD and CCD batch processes, theoretical model performance simulations were carried out with SWRO batch apparatus of same single-element (SWC6-MAX) module design under the same conditions of same feed source (10,000 ppm NaCl with 125 ppm silica), applied pressure (47 bar), initial flow rates (5.45 m^3/h module inlet; 3.00 m^3/h module outlet; and 2.45 m^3/h permeate), module recovery (MR = 45%); over 20 cycles of 82.85 ± 015% batch recovery at 25˚C under the same presumed pH (3–5) using the same antiscalant of the original OCD study [7]. The results of this theoretical study reveal milder batch process conditions for CCD compared with OCD of longer sequence duration (23.35 instead of 15.95 min), much lower energy consumption (1.57 instead of 7.93 kWh/m^3) with average TDS of permeates about the same for both processes up to ~75% batch recovery and higher for former process (531 instead of 316 ppm TDS) at the ultimate batch recovery (~83%) level and same pattern also repeated for the average Silica content in permeates (6.76 instead of 3.65 ppm silica). Silica in the recycled concentrates of both CCD and OCD processes is found in the range of 125–728 ± 6 ppm) and reveals desalination under high super-saturation conditions with silica maximum of ~5.8-fold (~580%) excess over the ordinary saturation level of silica.

The advantage of batch CCD over OCD revealed in the current study may suggest the effective use of the former process for volume reduction of difficult industrial effluents at large as well as to the effective use the consecutive sequential BWRO-CCD technology with module containing more than one element for high recovery desalination of rich Silica-containing brackish water sources.

Acknowledgments

Funds to *Desalitech Ltd*. by AQUAGRO FUND L.P. (Israel) and by Liberation Capital LLC (USA) are gratefully acknowledged.

References

[1] <http://vikipedia.org/viki/NEWater>.
[2] S. Loeb, Method and apparatus for generating power utilizing pressure-retarded-osmosis, US patent No. 3,906,250,1975.
[3] S. Loeb, Production of energy from concentrated brines by pressure-retarded osmosis, J. Membr. Sci. 1 (1976) 49–63.
[4] A. Tanioka, Power generation by pressure retarded osmosis using concentrated brine from seawater desalination system and treated sewage, review of experience with pilot in Japan, The 3rd Osmosis Membrane Summit, April 26–27, Barcelona, Spain, 2012.
[5] M. Kurihara, Government funded programs worldwide, the Japanese "Mega-ton Water System" project, The 3rd Osmosis Membrane Summit, April 26–27, Barcelona, Spain, 2012.
[6] K. Saito, M. Irie, S. Zaitsu, H. Sakai, H. Hayashi, A. Tanioka, Power generation with salinity gradient by pressure retarded osmosis using concentrated brine from SWRO system and treated sewage as pure water, Desalin. Water Treat. 41 (2012) 114–121.

[7] A.J. Tarquin, Sea water reverse osmosis systems to reduce concentrate volume prior to disposal, US Patent Application, Pub. No.: US 2011/0036775 A1.
[8] A. Efraty, R.N. Barak, Z. Gal, Closed circuit desalination—A new low energy high recovery technology without energy recovery, Desalin. Water Treat. 31 (2011) 95–101.
[9] A. Efraty, R.N. Barak, Z. Gal, Closed circuit desalination series no-2: New affordable technology for sea water desalination of low energy and high flux using short modules without need of energy recovery, Desalin. Water Treat. 42 (2012) 189–196.
[10] A. Efraty, Closed circuit desalination series no-6: conventional RO compared with the conceptually different new closed circuit desalination technology, Desalin. Water Treat. 41 (2012) 279–295.
[11] A. Efraty, Closed circuit desalination series no. 8: record saving of RO energy by SWRO-CCD without need of energy recovery, Desalin. Water Treat. 52(31–33) (2014) 5717–5730.
[12] IMS Design Integrated Membrane Solution Software. Available from: <http://membranes.com/index.php?pagename=imsdesign>.
[13] Specifications of the SWC6-MAX membrane element by Hydranautics. Available from: <http://www.membranes.com/docs/8inch/SWC6MAX.pdf>.
[14] Desalitech Ltd, unpublished results.